

# Interference Between Molecular and Photon Field-Mediated Electron Transfer Coupling Pathways in Cavities

Sutirtha N. Chowdhury,<sup>\*,†</sup> Peng Zhang,<sup>\*,†</sup> and David N. Beratan<sup>\*,‡</sup>

<sup>†</sup>Department of Chemistry, Duke University, Durham, North Carolina 27708, USA

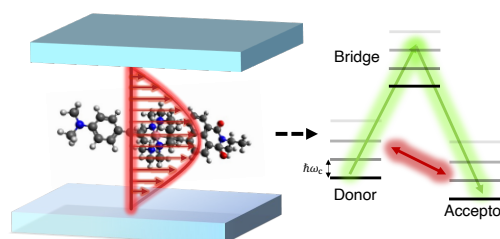
<sup>‡</sup>Department of Chemistry and Department of Physics, Duke University, Durham, North Carolina 27708, USA; Department of Biochemistry, Duke University, Durham, North Carolina 27710, USA

E-mail: sutirtha.chowdhury@duke.edu; peng.zhang@duke.edu; david.beratan@duke.edu

## Abstract

Cavity polaritonics is capturing the imagination of the chemistry community because of the novel opportunities it creates to direct chemistry. Electron transfer (ET) reactions are among the simplest reactions, and they also underpin bioenergetics. As such, new conceptual strategies to manipulate and direct electron flow at the nanoscale are of wide ranging interest in biochemistry, energy science, bio-inspired materials science, and chemistry. We show that optical cavities can modulate electron transfer pathway interferences and ET rates in donor-bridge-acceptor (DBA) systems. We derive the rate for DBA electron transfer systems when they are coupled with cavity photon fields (which may be off- or on-resonance with a molecular electronic transition), emphasizing novel cavity-induced pathway interferences with the molecular electronic coupling pathways, as these interferences allow a new kind of ET rate tuning. We also examined the ET kinetics for both low and high cavity frequency regimes as the light-matter coupling strength is varied. The interference between the cavity-induced and intrinsic molecular coupling pathway interference is defined by the cavity properties, including the cavity frequency and the light-matter coupling interaction strength. Thus, manipulating the cavity-induced interferences with the chemical coupling pathways offers new strategies to direct charge flow at the nanoscale.

Coupling molecular system to a photon field in an optical cavity allows new strategies to redirect chemistry.<sup>1–28</sup> Theory has played an important role in defining the principles of cavity quantum-electrodynamics (cQED) that enable new reactivities in a photon-molecule hybrid system. Despite encouraging progress, understanding electron transfer (ET) mechanisms in molecules coupled to an optical cavity



is challenging. Previous theoretical studies<sup>7,29–32</sup> addressed cavity effects on ET activation free energies and nonadiabatic interactions that arise when coupling the cavity mode to local donor excitations, or with the donor-to-acceptor transitions. These earlier studies indicate that ET rates can be altered significantly, through their effective Franck-Condon factors, when a molecule is coupled to a cavity.

Our goal is to understand how cavity interactions may modulate electron tunneling from donor to acceptor and, in particular, how the cavity may alter the coupling *pathway interference* in donor-bridge-acceptor (DBA) systems. In bridge-mediated ET with off-resonant bridges, the donor-acceptor coupling arises from a combination of through-bond and through-space interactions, and ET occurs via superexchange mediated by the many coupling pathways established by these interactions.<sup>33–36</sup> Interestingly, we find that the cavity modulates the effective donor-acceptor (DA) interaction and the nature of the interference between direct (cavity mediated) and superexchange coupling

pathways. Without light-matter coupling, we use a Marcus-like<sup>37</sup> nonadiabatic ET rate theory to describe the bridge-mediated ET. We further derive a rate expression in the weak coupling (nonadiabatic) limit for the hybrid cavity DBA system when the cavity mode is off- or on-resonance with molecular electronic transitions. In particular, we explore thermal ET in mixed valence (MV) DBA compounds when the cavity mode is resonantly coupled to the intervalence charge-transfer electronic excitation (IV-CT).<sup>38–41</sup> The IV-CT band is an optically induced charge transfer transition that shifts the electron from D to A.<sup>42–44</sup>

We find that the optical cavity creates a family of field-mediated donor-acceptor coupling pathways that interfere with the superexchange paths that are intrinsic to the DBA structure in the absence of the cavity. Importantly, the cavity tunes the strength of the interference between the two classes of coupling pathways. By changing the properties of the cavity, including the photon frequency, light-matter coupling strength, and quantum state of the photon, we show that one can plausibly suppress or enhance the rate of ET in DBA structures. This finding suggests the possibility of modulating coupling pathways and ET rates in optical cavities, creating a new strategy for ET rate manipulation.<sup>45</sup>

We use the Pauli-Fierz (PF) non-relativistic quantum electrodynamics (QED) Hamiltonian<sup>16,21,30,46,47</sup>  $\hat{H}_{\text{PF}}$  to describe the DBA system (electrons and nuclei)  $\hat{H}_{\text{M}}$  coupled to the radiation field  $\hat{H}_{\text{p}} = (\hat{a}^\dagger \hat{a} + \frac{1}{2})\hbar\omega_{\text{c}}$  through  $\hat{H}_{\text{int}}$ . For a molecule coupled to a single photon mode inside an optical cavity in the long wavelength limit,<sup>21</sup> the PF Hamiltonian is

$$\begin{aligned}\hat{H}_{\text{PF}} &= \hat{H}_{\text{M}} + \hat{H}_{\text{p}} + \hat{H}_{\text{int}} \quad (1) \\ &= \hat{H}_{\text{M}} + (\hat{a}^\dagger \hat{a} + \frac{1}{2})\hbar\omega_{\text{c}} + \hat{\boldsymbol{\chi}} \cdot \hat{\boldsymbol{\mu}} (\hat{a}^\dagger + \hat{a}) + \frac{(\hat{\boldsymbol{\chi}} \cdot \hat{\boldsymbol{\mu}})^2}{\hbar\omega_{\text{c}}} \\ &= \hat{H}_{\text{M}} + \frac{1}{2}\hat{P}_{\text{c}}^2 + \frac{1}{2}\omega_{\text{c}}^2 \left( \hat{Q}_{\text{c}} + \sqrt{\frac{2}{\hbar\omega_{\text{c}}^3}} \hat{\boldsymbol{\chi}} \cdot \hat{\boldsymbol{\mu}} \right)^2\end{aligned}$$

$\hat{a}^\dagger$  and  $\hat{a}$  are the photon creation and annihilation operators respectively.  $\hat{Q}_{\text{c}} = \sqrt{\hbar/2\omega_{\text{c}}}(\hat{a}^\dagger + \hat{a})$  and  $\hat{P}_{\text{c}} = i\sqrt{\hbar\omega_{\text{c}}}/2(\hat{a}^\dagger - \hat{a})$  are the photon coordinate and momentum operators, where  $\omega_{\text{c}}$  is the photon frequency in the cavity.  $\hat{H}_{\text{int}} = \hat{\boldsymbol{\chi}} \cdot \hat{\boldsymbol{\mu}} (\hat{a}^\dagger + \hat{a}) + \frac{(\hat{\boldsymbol{\chi}} \cdot \hat{\boldsymbol{\mu}})^2}{\hbar\omega_{\text{c}}}$  describes the light-matter interaction, where,  $\hat{\boldsymbol{\chi}} = \sqrt{\frac{\hbar\omega_{\text{c}}}{2\epsilon_0\mathcal{V}}}\hat{\mathbf{e}}$ . The unit vector  $\hat{\mathbf{e}}$  is along the polarization direction, and  $\mathcal{V}$  is the quantization volume for the cavity-photon field.  $\epsilon_0$  is the permittivity in the cavity. Finally,  $\hat{\boldsymbol{\mu}}$  is the molecular dipole operator (for both electrons and nuclei).

Previous findings indicate that the coupling with an optical cavity can significantly change ET rates by in-

fluencing the Franck-Condon factor.<sup>7,12,23–25,29–32,48–50</sup> However, prior studies did not explore how the cavity might alter the bridge-mediated (superexchange) couplings or their interferences with the direct cavity-mediated interaction between D and A. We study a DBA system coupled to one radiation mode in an optical cavity. The DBA molecular Hamiltonian  $\hat{H}_{\text{M}}$  is:

$$\begin{aligned}\hat{H}_{\text{M}} &= \hat{T}_{\text{s}} + \sum_i U_i |i\rangle \langle i| + V_{\text{DB}}(|\text{D}\rangle \langle \text{B}| + |\text{B}\rangle \langle \text{D}|) \quad (2) \\ &+ V_{\text{BA}}(|\text{B}\rangle \langle \text{A}| + |\text{A}\rangle \langle \text{B}|) + \sum_i \frac{1}{2} M_{\text{s}} \omega_{\text{s}}^2 (R_{\text{s}} - R_i^0)^2 |i\rangle \langle i| \\ &+ \hat{H}_{\text{sb}},\end{aligned}$$

where  $|i\rangle \in \{|\text{D}\rangle, |\text{B}\rangle, |\text{A}\rangle\}$  indexes the diabatic donor, bridge, and acceptor states,  $\hat{T}_{\text{s}} = \hat{P}_{\text{s}}^2/2M_{\text{s}}$  is the kinetic energy operator of the reaction coordinate,  $R_{\text{s}}$ , centered at  $R_i^0$ , with nuclear mass  $M_{\text{s}}$  and frequency  $\omega_{\text{s}}$ . Further,  $U_i$  is the (constant) diabatic state energy (site energy) associated with state  $|i\rangle$ .  $V_{\text{DB}}$  and  $V_{\text{BA}}$  are the constant diabatic couplings of donor with bridge and bridge with acceptor, respectively. The direct diabatic coupling between  $|\text{D}\rangle$  and  $|\text{A}\rangle$  is neglected *i.e.*,  $V_{\text{DA}} = V_{\text{AD}} = 0$  as the donor to acceptor distance is typically larger than 1 nm. The solvent reorganization energy is defined as  $\lambda_{\text{DA}} = \frac{1}{2} M_{\text{s}} \omega_{\text{s}}^2 (R_{\text{D}}^0 - R_{\text{A}}^0)^2$ . We take  $R_{\text{D}}^0 = 0$  and  $R_{\text{A}}^0 = \sqrt{2\lambda_{\text{DA}}/f_0}$ , where  $f_0$  is the force constant and  $\omega_{\text{s}} = \sqrt{f_0/M_{\text{s}}}$ . We used a solvent reorganization energy of  $\lambda_{\text{DA}} = 0.65$  eV and we assume degenerate donor and acceptor states. That is, the site-energy difference between donor and acceptor states is  $U_{\text{D}} - U_{\text{A}} = 0$ . Also, the site-energy difference between the (off resonance) bridge and the donor is  $\Delta E = U_{\text{B}} - U_{\text{D}} = 1.5$  eV.  $\hat{H}_{\text{sb}}$  is the system-bath interaction Hamiltonian.<sup>31</sup> The above molecular system Hamiltonian is characteristic of type-II MV compounds, where the effective DA coupling is less than the reorganization energy  $\lambda$ .<sup>38,41</sup>

For type-II MV structures of interest, we assume that both the transition and permanent dipole moments of the molecule are constant, *i.e.*, they are not a function of the solvent polarization coordinate. We assume that these dipoles are aligned with the cavity field polarization direction  $\hat{\mathbf{e}}$  and that the light field couples directly with the IV-CT electronic transition. Hence, the light-matter interaction is

$$\begin{aligned}\hat{\boldsymbol{\chi}} \cdot \hat{\boldsymbol{\mu}} &= \chi \mu_{\text{DA}} (|\text{D}\rangle \langle \text{A}| + |\text{A}\rangle \langle \text{D}|) + \chi \mu_{\text{DD}} |\text{D}\rangle \langle \text{D}| \\ &+ \chi \mu_{\text{AA}} |\text{A}\rangle \langle \text{A}| \quad (3)\end{aligned}$$

where,  $\chi = \sqrt{\frac{\hbar\omega_{\text{c}}}{2\epsilon_0\mathcal{V}}}$  and we further assume that both  $\hat{\boldsymbol{\chi}}$  and  $\hat{\boldsymbol{\mu}}$  are oriented along the cavity field polarization direction  $\hat{\mathbf{e}}$ . Using Eq. 3, the light-matter interaction

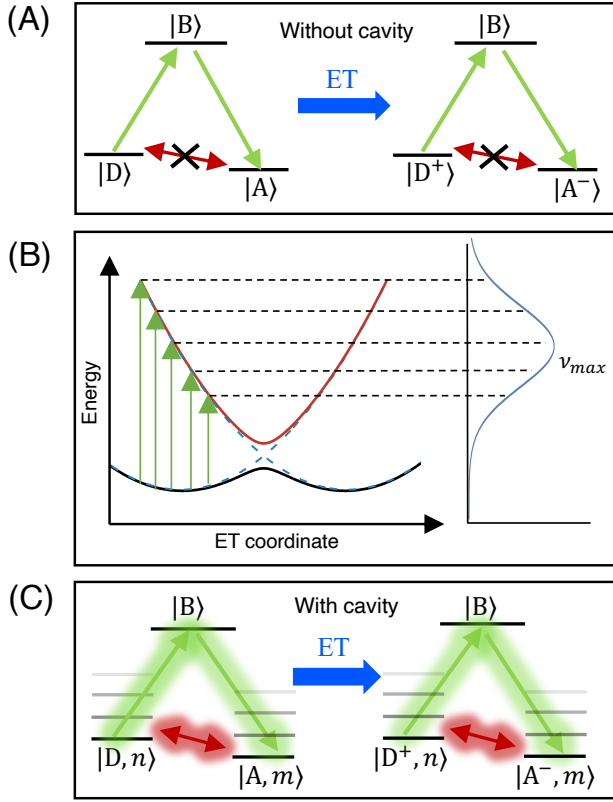


Figure 1: (A) Schematic energy landscape for a DBA-ET structure without a cavity. Electron tunneling from D to A through the bridge is described using an effective two-level Hamiltonian as illustrated in panel (B). Green arrows indicate bridge-mediated interactions, and no direct interactions are present without the cavity. (B) A typical potential energy surface for the IV-CT DBA complex and its absorption spectra, which are resonantly coupled with the cavity photon field.  $\nu_{max}$  is the frequency of the absorption band maxima. (C) Light-matter hybrid DBA structure, where  $|D, n\rangle$  and  $|A, m\rangle$  are the donor and acceptor photon dressed states, respectively. The green arrows represent the bridge-mediated interactions and the red arrow indicates the direct DA interactions in the light-matter hybrid manifold.

Hamiltonian  $\hat{H}_{int}$ , is

$$\hat{H}_{int} = \hbar g_c (|D\rangle\langle A| + |A\rangle\langle D|)(\hat{a}^\dagger + \hat{a}) + (\chi\mu_{DD}|D\rangle\langle D| + \chi\mu_{AA}|A\rangle\langle A|)(\hat{a}^\dagger + \hat{a}) + \frac{(\hat{\chi} \cdot \hat{\mu})^2}{\hbar\omega_c}, \quad (4)$$

where the coupling strength  $\hbar g_c \equiv \chi\mu_{DA}$ , and  $\frac{(\hat{\chi} \cdot \hat{\mu})^2}{\hbar\omega_c}$  is the dipole-self energy (DSE). Note that,  $\hat{\chi} \cdot \hat{\mu}$  has units of energy, and the unit of  $\hat{\chi}$  is energy/dipole moment. We set the transition and permanent dipole moment as unitless parameters (as we scaled by units of dipole moment in the denominator). In this model, we used the D to A transition dipole moment  $\mu_{DA} = 1$  and the permanent dipole moments  $\mu_{DD} = 5$  and  $\mu_{AA} = -5$ .

Figure 1 shows a typical DBA electron-transfer system with and without the cavity, and the associated IV-CT excitation. Without the cavity, ET is mediated by superexchange via one bridge state and by the direct through-space donor-acceptor electronic coupling interaction (Figure 1(A)). When the molecule is coupled to the cavity (Figure 1(C)), ET occurs via cavity-created light-matter hybrid states, such as  $|D, n\rangle$  (the donor state with  $n$  photons in the cavity), and  $|A, m\rangle$  (the acceptor state with  $m$  photons in the cavity). Each dressed channel is separated by the energy of the photon field  $\hbar\omega_c$  in the cavity. The bridge state is not dressed by the photon numbers, because the light field is only resonant with the  $|D\rangle \rightarrow |A\rangle$  IV-CT transition. In this cavity-enabled mechanism, ET occurs by (1) bridge-mediated superexchange ( $|D, n\rangle \rightarrow |B\rangle \rightarrow |A, m\rangle$ ), and (2) direct through-space donor to acceptor tunneling ( $|D, n\rangle \rightarrow |A, m\rangle$ ) mediated by cavity modes. These two classes of pathways provide very different rate profiles with respect to the light-matter interaction strength. Importantly, The ET rate depends on the interference between the superexchange and direct coupling pathways.

We use two analytical rate theories to quantify the ET rate constants for our dressed molecular system. Without the cavity, the ET rate is described by a non-adiabatic Marcus-like rate<sup>37,51</sup> With the cavity, the Fermi golden rule (FGR) description of the polaron mediated electron transfer (PMET) rate remains valid.<sup>7,29–32,48</sup>

**(1) Marcus-like nonadiabatic ET:** The rate for the DBA system, without the cavity is:

$$k_{MT} = \frac{2\pi|V_{DA}^{eff}|^2}{\hbar} \sqrt{\frac{1}{4\pi\lambda_{DA}k_B T}} \exp\left[-\frac{(\Delta G + \lambda_{DA})^2}{4\lambda_{DA}k_B T}\right], \quad (5)$$

where,  $V_{DA}^{eff}$  is the effective coupling between D and A diabatic states.

$$V_{DA}^{eff} = -\frac{V_{DB}V_{BA}}{2} \left[ \frac{1}{U_B - U_A} + \frac{1}{U_B - U_D} \right]. \quad (6)$$

$\Delta G = (U_A - U_D) - \frac{V_{BA}^2}{(U_B - U_A)} + \frac{V_{DB}^2}{(U_B - U_D)}$  is the effective ET driving force,  $\lambda_{DA}$  is the reorganization energy, where,  $k_B$  is Boltzmann's constant and  $T$  is the temperature ( $T = 300K$ ).

**(2) Fermi's golden rule for PMET:** We now describe the PMET rate when the photon frequency is resonant with the IV-CT band. PMET occurs from a set of photon-dressed donor states  $|D, n\rangle$  to a set of photon dressed acceptor states  $|A, m\rangle$  via a virtual bridge state  $|B\rangle$ , or via direct interaction between  $|D, n\rangle$  to  $|A, m\rangle$  states. To calculate the rates associated with each pho-

ton dressed channel for the two reaction pathways, we follow earlier approaches<sup>7,29–31</sup> and use Fermi's golden rule for the ET rates:<sup>52–54</sup>

$$k_{\text{FGR}} = \sum_n P_n \sum_m \frac{|F_{nm}|^2}{\hbar} \sqrt{\frac{\pi}{\lambda_{\text{DA}} k_B T}} \times \exp\left[-\frac{(\Delta G_{nm} + \lambda_{\text{DA}})^2}{4\lambda_{\text{DA}} k_B T}\right], \quad (7)$$

where  $F_{nm}$  is the effective DA coupling among photon dressed states

$$F_{nm} = \underbrace{\hbar g_c [\sqrt{n} S_{n-1,m}^{\text{DA}} + \sqrt{n+1} S_{n+1,m}^{\text{DA}}]}_{\text{direct DA coupling}} - \underbrace{\frac{\tilde{V}_{n,0}^{\text{DB}} \tilde{V}_{0,m}^{\text{BA}}}{2} \left[ \frac{1}{(U_B - U_A) - m\hbar\omega_c} + \frac{1}{(U_B - U_D) - n\hbar\omega_c} \right]}_{\text{bridge mediated coupling}} \quad (8)$$

with,  $\tilde{V}_{n,0}^{\text{DB}} = V_{\text{DB}} S_{n,0}^{\text{DB}}$ ,  $\tilde{V}_{0,m}^{\text{BA}} = V_{\text{BA}} S_{0,m}^{\text{BA}}$  and  $S_{nm}^{\text{DA}} = \langle n | e^{-i/\hbar \sqrt{2/\hbar\omega_c^3} \chi (\mu_{\text{DD}} - \mu_{\text{AA}}) \hat{P}_c} | m \rangle$ ,  $S_{n,0}^{\text{DB}} = \langle n | e^{-i/\hbar \sqrt{2/\hbar\omega_c^3} \chi \mu_{\text{DD}} \hat{P}_c} | 0 \rangle$ ,

and  $S_{0,m}^{\text{BA}} = \langle 0 | e^{i/\hbar \sqrt{2/\hbar\omega_c^3} \chi \mu_{\text{AA}} \hat{P}_c} | m \rangle$ . The derivations of Eq. 7 and Eq. 8, and the expressions for  $\Delta G_{nm}$  (the effective driving force between photon-dressed donor and acceptor states), are provided in the SI. The thermal population of the corresponding cavity mode is

$$P_n = \frac{\exp[-\beta n \hbar \omega_c]}{\sum_n \exp[-\beta n \hbar \omega_c]}, \quad (9)$$

where,  $\beta = 1/k_B T$ . We also derive the rate for the off-resonance case (where the cavity mode is not resonant with any electronic transitions). The effective DA couplings and the rate constants for the off-resonance theory appear in the SI.

We first describe the PMET (polariton mediated electron transfer) rate obtained from the FGR rate expression (Eq. 7) for on-resonance conditions. Figure 2 shows the computed PMET rates as a function of effective light-matter coupling ( $g_c/\omega_c$ ) strengths with  $\hbar\omega_c = 860$  meV (solid lines) and  $\hbar\omega_c = 430$  meV (dashed lines) at  $\Delta E = 1.5$  eV. The colored lines represent  $V_{\text{DB}}$  and  $V_{\text{BA}}$  couplings:  $V_{\text{DB}} = V_{\text{BA}} = 0.02$  eV (black),  $V_{\text{DB}} = V_{\text{BA}} = 0.04$  eV (green), and  $V_{\text{DB}} = V_{\text{BA}} = 0.06$  eV (orange). When the molecule is decoupled from the cavity, the ET occurs via  $|D\rangle \rightarrow |B\rangle \rightarrow |A\rangle$  superexchange and the rate is analyzed using Eq. 5.

In the presence of a cavity, ET is mediated by two classes of coupling pathways

- **Pathway 1:** ET from photon dressed donor states  $|D, n\rangle$  to photon dressed acceptor states  $|A, m\rangle$  via a single bridge state  $|B\rangle$  (the bridge

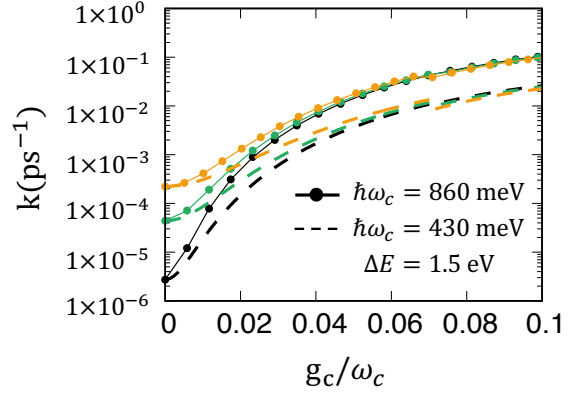


Figure 2: PMET rates constants computed for a range of effective light-matter coupling strengths ( $g_c/\omega_c$ ). The solid lines correspond to  $\hbar\omega_c = 860$  meV and the dashed lines to  $\hbar\omega_c = 430$  meV. The colors represent different  $V_{\text{DB}}$  and  $V_{\text{BA}}$  values:  $V_{\text{DB}} = V_{\text{BA}} = 0.02$  eV (black),  $V_{\text{DB}} = V_{\text{BA}} = 0.04$  eV (green), and  $V_{\text{DB}} = V_{\text{BA}} = 0.06$  eV (orange). The smaller the  $V_{\text{DB}}$  and  $V_{\text{BA}}$  values, the larger the PMET rate enhancement is found to be.

is not coupled with the light-field).

- **Pathway 2:** ET from direct transitions between  $|D, n\rangle$  and  $|A, m\rangle$ . This direct transition is determined by cavity properties, such as the light-matter coupling strengths and the photon frequency.

First, one finds that increasing  $g_c/\omega_c$  causes the reaction rate to grow compared to the cavity free situation (when  $g_c/\omega_c = 0$ ). This is found because increasing the light-matter coupling strength causes the ET to occur mostly via direct transitions between  $|D, n\rangle$  and  $|A, m\rangle$  (pathway 2); the direct coupling is proportional to the light-matter coupling strength, which is understood through Eq. 8. The first term in Eq. 8 grows with increasing light-matter coupling strength.

Second, the rate enhancement described above decreases as  $V_{\text{DB}}$  and  $V_{\text{BA}}$  couplings grow (see the black dashed/solid line and orange dashed/solid line). This finding is understood by considering the destructive interference (see Eq. 8) that arises between the bridge-mediated superexchange coupling (pathway 1), and the direct (through-space) DA coupling (pathway 2). Increasing  $V_{\text{DB}}$  and  $V_{\text{BA}}$  causes the bridge-mediated pathway to interfere strongly with the direct (through-space) coupling from D to A, so the rate enhancement is reduced compared with the case of smaller  $V_{\text{DB}}$  and  $V_{\text{BA}}$  values.

Third, in this model, the PMET rate is larger for high cavity frequencies. The rate is nearly one order of magnitude larger when  $\hbar\omega_c = 860$  meV compared to  $\hbar\omega_c =$

430 meV. This effect can also be understood as arising from coupling pathway interferences. The smaller the photon frequency, the higher energy donor dressed states ( $|D, n\rangle$ ) are thermally populated, and there will be larger interactions of donor-dressed states with the bridge state, producing stronger destructive pathway interferences and slower ET rates. Interestingly, the cavity frequency modulated PMET rate enhancement also depends on the ET driving force ( $-\Delta G_{nm}$ ). Previous studies<sup>30,31</sup> found that the PMET rate is significantly enhanced by a low cavity frequency in the Marcus normal regime. One observes this effect by computing the PMET rate as a function of the molecular driving force, and this finding is also consistent with the DBA model system analysis.

PMET rates may be measured using methods reported earlier,<sup>40</sup> for example through the IR spectral broadening of Ru(II/III) mixed-valence complexes. Further, it is well known that ET couplings and reorganization energies can be derived from intervalence spectra in the weak DA coupling limit.<sup>38,40,42–44</sup> Analogous measurement of intervalence spectra can provide information on how the donor-acceptor couplings are influenced when the cavity mode is resonantly coupled with the IV-CT absorption band.

In addition to the resonant treatment describe above, we also developed an off-resonance rate theory for PMET (see SI). In this regime, the D, B, and A states couple with the photon field. Figure 3 shows the computed PMET rate found for the off-resonance regime. In this case, ET occurs from photon dressed donor states  $|D, n\rangle$  to photon dressed acceptor states  $|A, m\rangle$  via bridge-mediated channels  $|B, l\rangle$  ( $|D, n\rangle \rightarrow |B, l\rangle \rightarrow |A, m\rangle$ ) and also direct transition from  $|D, n\rangle \rightarrow |A, m\rangle$  channels (see Figure 3(A)). The key difference, relative to the resonant theory, is the contribution of the many-fold virtual bridge states that produce stronger destructive interferences. Figure 3(A) shows the light-matter hybrid DBA-ET energy landscape for off-resonance superexchange. Figure 3(B) and 3(C) show the computed reaction rate as a function of the effective light-matter coupling ( $g_c/\omega_c$ ) at  $\Delta E = 1.5$  eV for  $\hbar\omega_c = 200$  meV and  $\hbar\omega_c = 40$  meV. Details of the model Hamiltonian and additional parameters appear in the SI. Each panel shows three different rate signatures, (a) the ET rate from D to A,  $k_{\text{total}}$ , (b) the ET rate for just the direct (through-space) D-A transition,  $k_{\text{direct}}$ , (calculated using only the direct coupling term (see Eq. S19 in the SI)), and (c) the ET rate for just bridge mediated (superexchange) coupling,  $k_{\text{bridge}}$ , (calculated using only the bridge mediated coupling (see Eq. S20 of the SI)). In Figures 3(B) and 3(C), the initial rate suppression is

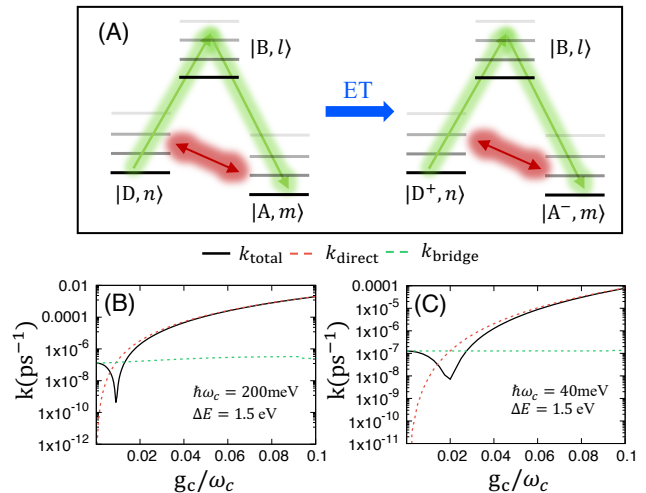


Figure 3: (A) DBA cavity-hybrid model system, where the cavity mode is off of resonance with the DBA electronic transition.  $|D, n\rangle$ ,  $|B, l\rangle$ , and  $|A, m\rangle$  are the photon dressed donor, bridge and acceptor states, respectively. (B) PMET rate constants calculated over a range of effective light-matter coupling strengths ( $g_c/\omega_c$ ) with  $\hbar\omega_c = 200$  meV and (C)  $\hbar\omega_c = 40$  meV. The solid black line corresponds to the total rate, the orange dashed line refers only to the cavity established direct (through-space) donor-to-acceptor rate, and the dashed green line represents the bridge assisted (superexchange) rate.

followed by a rate enhancement. This feature is explained by considering interference between the two coupling paths. Weaker light-matter couplings cause the direct and the bridge-mediated paths to interfere strongly, producing rate suppression. Further increasing the effective light-matter coupling ( $g_c/\omega_c$ ),  $k_{\text{direct}}$  dominates over  $k_{\text{bridge}}$  and the overall ET rate is enhanced. The rate suppression is broader for Figure 3(C) compared to Figure 3(B). This behavior arises since, at the lower photon frequency of Figure 3(C), the high lying donor states are thermally populated. These states thus participate in the ET process, and they produce stronger interactions with bridge states. Hence, the enhancement of  $k_{\text{direct}}$  is weaker for Figure 3(C), leading to a broader suppression as a function of  $g_c/\omega_c$ , and the  $k_{\text{direct}}$  value is almost an order of magnitude smaller, explaining the faster growth of  $k_{\text{direct}}$  in Figure 3(B) compared to 3(C). This produces two different light-matter coupling modulated ET rates in Fig. 3(B) and 3(C).

We developed PMET rate theories for DBA systems in the limit of on-resonance coupling (where the photon mode is resonant with the IV-CT band) and off-resonance coupling. The computed PMET rates indicate that rate modulation occurs via two coupling pathways: (a) through space paths (cavity created, direct  $|D\rangle \rightarrow |A\rangle$  transition) and (b) through-bond paths

(cavity modulated  $|D\rangle \rightarrow |B\rangle \rightarrow |A\rangle$  transitions). We found that ET rates can be suppressed or enhanced as a function of the effective light-matter coupling strength. This rate control is largely determined by the cavity modulated interference between the through-space and through-bond coupling pathways. This perspective on cavity-modulated coupling pathway interferences points to a novel approach for modulating charge flow through molecules in cavities, supplementing earlier strategies.<sup>7,29–31</sup>

This study reveals the quantum pathway interference analysis for DBA structures in a cavity. PMET is predicted to enable the tuning of ET kinetics by manipulating the interference between through-bond and through-space coupling pathways in cavities, and this approach is anticipated to provide novel strategies to manipulate the polariton chemistry of ET systems.

Having a strategy to manipulate coupling pathway interference may also lead to new approaches to control chemical reactivity by coupling the vibrational degrees of freedom with the radiation field, specifically in the strong vibrational coupling and nonadiabatic limits.

## Acknowledgments

The authors thank the National Science Foundation (CHE-1954853) for support of this research.

## Supporting Information Available

The Supporting Information is available free of charge on the ACS Publications website.

Model system and parameters for the off resonance Hamiltonian, detailed derivation of the off-resonance rate theory, detailed derivation of the on-resonance rate theory, and additional numerical results.

## References

- (1) Hutchison, J. A.; Schwartz, T.; Genet, C.; Devaux, E.; Ebbesen, T. W. Modifying Chemical Landscapes by Coupling to Vacuum Fields. *Angew. Chem. Int. Ed.* **2012**, *51*, 1592–1596.
- (2) Thomas, A.; Lethuillier-Karl, L.; Nagarajan, K.; Vergauwe, R. M. A.; George, J.; Chervy, T.; Shalabney, A.; Devaux, E.; Genet, C.; Moran, J.; Ebbesen, T. W. Tilting a Ground-State Reactivity Landscape by Vibrational Strong Coupling. *Science* **2019**, *363*, 615–619.
- (3) Thomas, A.; Jayachandran, A.; Lethuillier-Karl, L.; Vergauwe, R. M.; Nagarajan, K.; Devaux, E.; Genet, C.; Moran, J.; Ebbesen, T. W. Ground State Chemistry Under Vibrational Strong Coupling: Dependence of Thermodynamic Parameters on the Rabi Splitting Energy. *Nanophotonics* **2020**, *9*, 249 – 255.
- (4) Kowalewski, M.; Bennett, K.; Mukamel, S. Cavity Femtochemistry: Manipulating Nonadiabatic Dynamics at Avoided Crossings. *J. Phys. Chem. Lett.* **2016**, *7*, 2050–2054.
- (5) Kowalewski, M.; Bennett, K.; Mukamel, S. Non-Adiabatic Dynamics of Molecules in Optical Cavities. *J. Chem. Phys.* **2016**, *144*, 054309.
- (6) Feist, J.; Galego, J.; Garcia-Vidal, F. J. Polaritonic Chemistry with Organic Molecules. *ACS Photonics* **2018**, *5*, 205–216.
- (7) Herrera, F.; Spano, F. C. Cavity-Controlled Chemistry in Molecular Ensembles. *Phys. Rev. Lett.* **2016**, *116*, 238301.
- (8) Triana, J. F.; Peláez, D.; Sanz-Vicario, J. L. Entangled Photonic-Nuclear Molecular Dynamics of LiF in Quantum Optical Cavities. *J. Phys. Chem. A* **2018**, *122*, 2266–2278.
- (9) Mandal, A.; Huo, P. Investigating New Reactivities Enabled by Polariton Photochemistry. *J. Phys. Chem. Lett.* **2019**, *10*, 5519–5529.
- (10) Du, M.; Ribeiro, R. F.; Yuen-Zhou, J. Remote Control of Chemistry in Optical Cavities. *Chem* **2019**, *5*, 1167 – 1181.
- (11) Gu, B.; Mukamel, S. Manipulating Nonadiabatic Conical Intersection Dynamics by Optical Cavities. *Chem. Sci.* **2020**, *11*, 1290–1298.
- (12) Galego, J.; Climent, C.; Garcia-Vidal, F. J.; Feist, J. Cavity Casimir-Polder Forces and Their Effects in Ground-State Chemical Reactivity. *Phys. Rev. X* **2019**, *9*, 021057.
- (13) Hoffmann, N. M.; Schäfer, C.; Säkkinen, N.; Rubio, A.; Appel, H.; Kelly, A. Light-matter interactions via the exact factorization approach. *Eur. Phys. J. B* **2018**, *151*, 180.
- (14) Bennett, K.; Kowalewski, M.; Mukamel, S. Novel Photochemistry of Molecular Polaritons in Optical Cavities. *Faraday Discuss.* **2016**, *194*, 259–282.

- (15) Fregoni, J.; Granucci, G.; Coccia, E.; Persico, M.; Corni, S. Manipulating Azobenzene Photoisomerization Through Strong Light-Molecule Coupling. *Nat. Commun.* **2018**, *9*, 4688.
- (16) Vendrell, O. Coherent Dynamics in Cavity Femtochemistry: Application of the Multi-Configuration Time-Dependent Hartree Method. *Chem. Phys.* **2018**, *509*, 55–65.
- (17) Csehi, A.; Kowalewski, M.; Halász, G. J.; Vibók, Á. Ultrafast Dynamics in the Vicinity of Quantum Light-Induced Conical Intersections. *New J. Phys.* **2019**, *21*, 093040.
- (18) Szidarovszky, T.; Halász, G. J.; Császár, A. G.; Cederbaum, L. S.; Vibók, A. Conical Intersections Induced by Quantum Light: Field-Dressed Spectra from the Weak to the Ultrastrong Coupling Regimes. *J. Phys. Chem. Lett.* **2018**, *9*, 6215–6223.
- (19) Groenhof, G.; Toppari, J. J. Coherent Light Harvesting Through Strong Coupling to Confined Light. *J. Phys. Chem. Lett.* **2018**, *9*, 4848–4851.
- (20) Groenhof, G.; Climent, C.; Feist, J.; Morozov, D.; Toppari, J. J. Tracking Polariton Relaxation With Multiscale Molecular Dynamics Simulations. *J. Phys. Chem. Lett.* **2019**, *10*, 5476–5483.
- (21) Rokaj, V.; Welakuh, D. M.; Ruggenthaler, M.; Rubio, A. Light–Matter Interaction in the Long-wavelength Limit: No Ground-State Without Dipole Self-Energy. *J. Phys. B: At. Mol. Opt. Phys.* **2018**, *51*, 034005.
- (22) Li, T. E.; Tao, Z.; Hammes-Schiffer, S. Semiclassical Real-time Nuclear-electronic Orbital Dynamics for Molecular Polaritons: Unified theory of Electronic and Vibrational Strong Couplings. *J. Chem. Theory Comput.* **2022**, *18*, 2774–2784.
- (23) Xinyang, L.; Arkajit, M.; Pengfei, H. Cavity Frequency-Dependent Theory for Vibrational Polariton Chemistry. *Nat. comm.* **2021**, *12*, 1315.
- (24) Xinyang, L.; Arkajit, M.; Pengfei, H. Theory of Mode-Selective Chemistry through Polaritonic Vibrational Strong Coupling. *J. Phys. Chem. Lett.* **2021**, *12*, 6974–6982.
- (25) Arkajit, M.; Xinyang, L.; Pengfei, H. Theory of Vibrational Polariton Chemistry in the Collective Coupling Regime. *J. Chem. Phys.* **2022**, *156*, 014101.
- (26) Engelhardt, G.; Cao, J. Unusual Dynamical Properties of Disordered Polaritons in Microcavities. *Phys. Rev. B* **2022**, *105*, 064205.
- (27) Lindoy, L. P.; Mandal, A.; Reichman, D. R. Resonant Cavity Modification of Ground-State Chemical Kinetics. *J. Phys. Chem. Lett.* **2022**, *13*, 6580–6586.
- (28) Sun, J.; Vendrell, O. Suppression and Enhancement of Thermal Chemical Rates in a Cavity. *J. Phys. Chem. Lett.* **2022**, *13*, 4441–4446.
- (29) Semenov, A.; Nitzan, A. Electron Transfer in Confined Electromagnetic Fields. *J. Chem. Phys.* **2019**, *150*, 174122.
- (30) Mandal, A.; Krauss, T. D.; Huo, P. Polariton-Mediated Electron Transfer via Cavity Quantum Electrodynamics. *J. Phys. Chem. B* **2020**, *124*, 6321–6340.
- (31) Chowdhury, S. N.; Mandal, A.; Huo, P. Ring Polymer Quantization of the Photon Field in Polariton Chemistry. *J. Chem. Phys.* **2021**, *154*, 044109.
- (32) Saller, M. A. C.; Lai, Y.; Geva, E. An Accurate Linearized Semiclassical Approach for Calculating Cavity-Modified Charge Transfer Rate Constants. *J. Chem. Phys.* **2022**, *13*, 2330–2337.
- (33) Beratan, D. N. Why Are DNA and Protein Electron Transfer So Different? *Annu. Rev. Phys. Chem.* **2019**, *70*, 71–97.
- (34) Balabin, I. A.; Beratan, D. N.; Skourtis, S. S. Persistence of Structure Over Fluctuations in Biological Electron-Transfer Reactions. *Phys. Rev. Lett.* **2008**, *101*, 158102.
- (35) Skourtis, S. S. Probing Protein Electron Transfer Mechanisms From the Molecular to the Cellular Length Scales. *Biopolymers* **2013**, *100*, 82–92.
- (36) Gray, H. B.; Winkler, J. R. Electron Tunneling Through Proteins. *Q. Rev. Biophys.* **2003**, *36*, 341–372.
- (37) Marcus, R. A. On the Theory of Oxidation-Reduction Reactions Involving Electron Transfer. I. *J. Chem. Phys.* **1956**, *24*, 966–978.
- (38) Heckmann, A.; Lambert, C. Organic Mixed-Valence Compounds: A Playground for Electrons

- and Holes. *Angew. Chem. Int. Ed.* **2012**, *51*, 326–392.
- (39) Dereka, B.; Rosspeintner, A.; Li, Z.; Liska, R.; Vauthey, E. Direct Visualization of Excited-State Symmetry Breaking Using Ultrafast Time-Resolved Infrared Spectroscopy. *J. Am. Chem. Soc.* **2016**, *138*, 4643–4649.
- (40) Londergan, C. H.; Salsman, J. C.; Ronco, S.; Dolkas, L. M.; Kubiak, C. P. Solvent Dynamical Control of Electron-Transfer Rates in Mixed-Valence Complexes Observed by Infrared Spectral Line Shape Coalescence. *J. Am. Chem. Soc.* **2002**, *124*, 6236–6237.
- (41) Launay, J.-P. Mixed-Valent Compounds and their Properties – Recent Developments. *Eur. J. Inorg. Chem.* **2020**, *2020*, 329–341.
- (42) Hush, N. S. Homogeneous and heterogeneous optical and thermal electron transfer. *Electrochim. Acta* **1968**, *13*, 1005–1023.
- (43) Hopfield, J. Photo-induced charge transfer. A critical test of the mechanism and range of biological electron transfer processes. *Biophys. J.* **1977**, *18*, 311–321.
- (44) Richardson, D. E.; Taube, H. Mixed-valence molecules: electronic delocalization and stabilization. *Coord. Chem. Rev.* **1984**, *60*, 107–129.
- (45) Skourtis, S. S.; Waldeck, D. H.; Beratan, D. N. Fluctuations in biological and bioinspired electron-transfer reactions. *Annu. Rev. Phys. Chem.* **2010**, *61*, 461.
- (46) Cohen-Tannoudji, C.; Dupont-Roc, J.; Grynberg, G. Photons and Atoms: Introduction to Quantum Electrodynamics. *John Wiley & Sons, Inc.: Hoboken, U.S.A.* **1989**,
- (47) Flick, J.; Ruggenthaler, M.; Appel, H.; Rubio, A. Atoms and Molecules in Cavities, From Weak to Strong Coupling in Quantum-Electrodynamics (QED) Chemistry. *Proc. Natl. Acad. Sci. U. S. A.* **2017**, *114*, 3026–3034.
- (48) Campos-Gonzalez-Angulo, J. A.; Ribeiro, R. F.; Yuen-Zhou, J. Resonant Catalysis of Thermally Activated Chemical Reactions With Vibrational Polaritons. *Nat. Commun.* **2019**, *10*, 4685.
- (49) Yang, P.-Y.; Cao, J. Quantum Effects in Chemical Reactions Under Polaritonic Vibrational Strong Coupling. *J. Phys. Chem. Lett.* **2021**, *12*, 9531–9538.
- (50) Du, M.; Campos-Gonzalez-Angulo, J. A.; Yuen-Zhou, J. Nonequilibrium Effects of Cavity Leakage and Vibrational Dissipation in Thermally Activated Polariton Chemistry. *J. Chem. Phys.* **2021**, *154*, 084108.
- (51) Marcus, R. A.; Sutin, N. Electron Transfers in Chemistry and Biology. **1985**, *811*, 265–322.
- (52) Nitzan, A.; Jortner, J.; Rentzepis, P. M.; Porter, G. Intermediate Level Structure in Highly Excited Electronic States of Large Molecules. *Proc. R. Soc. London, Ser. A* **1972**, *327*, 367–391.
- (53) Ulstrup, J.; Jortner, J. The Effect of Intramolecular Quantum Modes on Free Energy Relationships for Electron Transfer Reactions. *J. Chem. Phys.* **1975**, *63*, 4358–4368.
- (54) Efrima, S.; Bixon, M. On the Role of Vibrational Excitation in Electron Transfer Reactions With Large Negative Free Energies. *Chem. Phys. Lett.* **1974**, *25*, 34–37.



# Supporting Information: Interference Between Molecular and Photon Field-mediated Electron Transfer Coupling Pathways in Cavities

Sutirtha N. Chowdhury,<sup>\*,†</sup> Peng Zhang,<sup>\*,†</sup> and David N. Beratan<sup>\*,‡</sup>

<sup>†</sup>*Department of Chemistry, Duke University, 3236 French Science Center, 124 Science Drive, Durham, North Carolina 27708, USA*

<sup>‡</sup>*Department of Chemistry and Department of Physics, Duke University, Durham, North Carolina 27708, USA; Department of Biochemistry, Duke University, Durham, North Carolina 27710, USA*

E-mail: sutirtha.chowdhury@duke.edu; peng.zhang@duke.edu; david.beratan@duke.edu

## Model Hamiltonian for the Off-Resonance Rate Theory

In this section, we describe the model Hamiltonian used to describe a light-matter hybrid DBA system in off resonance conditions. As with the on resonance condition (see main text), we also begin with the Pauli-Fierz (PF) Hamiltonian.

$$\begin{aligned}\hat{H}_{\text{PF}} &= \hat{H}_{\text{M}} + \hat{H}_{\text{P}} + \hat{H}_{\text{int}} \\ &= \hat{H}_{\text{M}} + (\hat{a}^\dagger \hat{a} + \frac{1}{2})\hbar\omega_c + \hat{\chi} \cdot \hat{\mu}(\hat{a}^\dagger + \hat{a}) + \frac{(\hat{\chi} \cdot \hat{\mu})^2}{\hbar\omega_c},\end{aligned}\tag{S1}$$

where  $\hat{a}$  and  $\hat{a}^\dagger$  are the photon creation and annihilation operator.  $\omega_c$  is the photon frequency in the cavity and  $\hat{H}_{\text{int}}$  is the light-matter interaction Hamiltonian:

$$\hat{H}_{\text{int}} = \hat{\chi} \cdot \hat{\mu}(\hat{a}^\dagger + \hat{a}) + \frac{(\hat{\chi} \cdot \hat{\mu})^2}{\hbar\omega_c}\tag{S2}$$

Under off resonance conditions, the donor ( $|D\rangle$ ), bridge ( $|B\rangle$ ), and acceptor ( $|A\rangle$ ) states are all coupled with the light field and the light-matter interaction term is written:

$$\begin{aligned} \hat{\chi} \cdot \hat{\boldsymbol{\mu}} = & \chi\mu_{DB}(|D\rangle\langle B| + |B\rangle\langle D|) + \chi\mu_{BA}(|B\rangle\langle A| + |A\rangle\langle B|) + \chi\mu_{DD}|D\rangle\langle D| \\ & + \chi\mu_{BB}|B\rangle\langle B| + \chi\mu_{AA}|A\rangle\langle A| \end{aligned} \quad (\text{S3})$$

where,  $\chi = \sqrt{\frac{\hbar\omega_c}{2\varepsilon_0V}}$ . We set  $\mu_{DA} = \mu_{AD} = 0$ , as charge transfer band absorption is typically weak. Using the Eq. S3 the  $\hat{H}_{\text{int}}$  term is:

$$\begin{aligned} \hat{H}_{\text{int}} = & \hbar g_c(|D\rangle\langle B| + |B\rangle\langle D|)(\hat{a}^\dagger + \hat{a}) + \hbar\eta_c(|B\rangle\langle A| + |A\rangle\langle B|)(\hat{a}^\dagger + \hat{a}) \\ & + (\chi\mu_{DD}|D\rangle\langle D| + \chi\mu_{BB}|B\rangle\langle B| + \chi\mu_{AA}|A\rangle\langle A|)(\hat{a}^\dagger + \hat{a}) + \frac{(\hat{\chi} \cdot \hat{\boldsymbol{\mu}})^2}{\hbar\omega_c}, \end{aligned} \quad (\text{S4})$$

where the coupling strength  $\hbar g_c \equiv \chi\mu_{DB}$ ,  $\hbar\eta_c \equiv \chi\mu_{BA}$ . In this light-matter hybrid system, we took  $\mu_{DB} = \mu_{BA} = 1$ , and the permanent dipole moment differences are  $\mu_{DD} - \mu_{AA} = 1$ ,  $\mu_{DD} - \mu_{BB} = 5$ , and  $\mu_{BB} - \mu_{AA} = 5$ . We treat the transition and permanent dipole moments as unitless numbers, but  $\hat{\chi} \cdot \hat{\boldsymbol{\mu}}$  has units of energy, and the DBA molecular Hamiltonian  $\hat{H}_M$  is the same as in Eq. (2) of the main text. The model parameters for  $\hat{H}_M$  are exactly the same as in the on-resonance case (see main text), except that we set  $V_{DB} = V_{BA} = 5$  meV, and the site energy difference between donor and acceptor states is  $U_D - U_A = 150$  meV.

### Derivation of the PMET Rate Theory for the Off-Resonance Case

We use the following polaron transformation operator<sup>??</sup> of the photonic degrees of freedom (DOF)

$$\hat{U}_{\text{pol}} = \exp \left[ \frac{i}{\hbar} \sqrt{\frac{2}{\hbar\omega_c^3}} \chi \sum_{j \in D, B, A} \mu_{jj} |j\rangle\langle j| \hat{P}_c \right]. \quad (\text{S5})$$

The polaron transformation operator shifts the photonic coordinate,  $e^{-\frac{i}{\hbar}Q_0\hat{P}_c}\hat{O}(\hat{Q}_c)e^{\frac{i}{\hbar}Q_0\hat{P}_c} = \hat{O}(\hat{Q}_c - Q_0)$ .  $\hat{U}_{\text{pol}}$  transforms  $|D\rangle\langle B|$  as follows:

$$\hat{U}_{\text{pol}}^\dagger |D\rangle\langle B| \hat{U}_{\text{pol}} = e^{-\frac{i}{\hbar}\sqrt{\frac{2}{\hbar\omega_c^3}}\chi(\mu_{\text{DD}} - \mu_{\text{BB}})\hat{P}_c} |D\rangle\langle B|.$$

This can be shown (with  $\hat{\Pi}_c = \frac{1}{\hbar}\sqrt{\frac{2}{\hbar\omega_c^3}}\chi\hat{P}_c$ ) as follows:

$$\begin{aligned} \hat{U}_{\text{pol}}^\dagger |D\rangle\langle B| \hat{U}_{\text{pol}} &= e^{-i\hat{\Pi}_c(\mu_{\text{DD}}|D\rangle\langle D| + \mu_{\text{BB}}|B\rangle\langle B| + \mu_{\text{AA}}|A\rangle\langle A|)} |D\rangle\langle B| e^{i\hat{\Pi}_c(\mu_{\text{DD}}|D\rangle\langle D| + \mu_{\text{BB}}|B\rangle\langle B| + \mu_{\text{AA}}|A\rangle\langle A|)} \\ &= e^{-i\hat{\Pi}_c\mu_{\text{DD}}|D\rangle\langle D|} e^{-i\hat{\Pi}_c\mu_{\text{BB}}|B\rangle\langle B|} e^{-i\hat{\Pi}_c\mu_{\text{AA}}|A\rangle\langle A|} |D\rangle\langle B| e^{i\hat{\Pi}_c\mu_{\text{DD}}|D\rangle\langle D|} e^{i\hat{\Pi}_c\mu_{\text{BB}}|B\rangle\langle B|} e^{i\hat{\Pi}_c\mu_{\text{AA}}|A\rangle\langle A|} \\ &= e^{-i\hat{\Pi}_c\mu_{\text{DD}}|D\rangle\langle D|} e^{-i\hat{\Pi}_c\mu_{\text{BB}}|B\rangle\langle B|} \left[ \hat{\mathbf{1}}_e - i\hat{\Pi}_c\mu_{\text{AA}}|A\rangle\langle A| + \dots \right] |D\rangle\langle B| \left[ \hat{\mathbf{1}}_e + i\hat{\Pi}_c\mu_{\text{DD}}|D\rangle\langle D| + \dots \right] \\ &\quad \times e^{i\hat{\Pi}_c\mu_{\text{BB}}|B\rangle\langle B|} e^{i\hat{\Pi}_c\mu_{\text{AA}}|A\rangle\langle A|} \\ &= e^{-i\hat{\Pi}_c\mu_{\text{DD}}|D\rangle\langle D|} e^{-i\hat{\Pi}_c\mu_{\text{BB}}|B\rangle\langle B|} |D\rangle\langle B| e^{i\hat{\Pi}_c\mu_{\text{BB}}|B\rangle\langle B|} e^{i\hat{\Pi}_c\mu_{\text{AA}}|A\rangle\langle A|} \\ &= e^{-i\hat{\Pi}_c\mu_{\text{DD}}|D\rangle\langle D|} \left[ \hat{\mathbf{1}}_e - i\hat{\Pi}_c\mu_{\text{BB}}|B\rangle\langle B| + \dots \right] |D\rangle\langle B| \left[ \hat{\mathbf{1}}_e + i\hat{\Pi}_c\mu_{\text{BB}}|B\rangle\langle B| + \dots \right] e^{i\hat{\Pi}_c\mu_{\text{AA}}|A\rangle\langle A|} \\ &= e^{-i\hat{\Pi}_c\mu_{\text{DD}}|D\rangle\langle D|} |D\rangle\langle B| e^{i\hat{\Pi}_c\mu_{\text{BB}}|B\rangle\langle B|} e^{i\hat{\Pi}_c\mu_{\text{AA}}|A\rangle\langle A|} \\ &= e^{i\hat{\Pi}_c\mu_{\text{BB}}|B\rangle\langle B|} \left[ \hat{\mathbf{1}}_e - i\hat{\Pi}_c\mu_{\text{DD}}|D\rangle\langle D| + \dots \right] |D\rangle\langle B| \left[ \hat{\mathbf{1}}_e + i\hat{\Pi}_c\mu_{\text{AA}}|A\rangle\langle A| + \dots \right] \\ &= e^{i\hat{\Pi}_c\mu_{\text{BB}}|B\rangle\langle B|} e^{-i\hat{\Pi}_c\mu_{\text{DD}}|D\rangle\langle D|} |D\rangle\langle B| = e^{-i\hat{\Pi}_c(\mu_{\text{DD}} - \mu_{\text{BB}})} |D\rangle\langle B| \end{aligned} \quad (\text{S6})$$

In the second line of Eq. S6, we used  $[|A\rangle\langle A|, |D\rangle\langle D|] = [|B\rangle\langle B|, |D\rangle\langle D|] = [|B\rangle\langle B|, |A\rangle\langle A|] = 0$  to split an exponential operator into two parts :  $e^{\hat{X} + \hat{Y}} = e^{\hat{X}} e^{\hat{Y}}$  when  $[\hat{X}, \hat{Y}] = 0$ . Following the same procedure, we find:

$$\hat{U}_{\text{pol}}^\dagger |B\rangle\langle D| \hat{U}_{\text{pol}} = e^{-\frac{i}{\hbar}\sqrt{\frac{2}{\hbar\omega_c^3}}\chi(\mu_{\text{BB}} - \mu_{\text{DD}})\hat{P}_c} |B\rangle\langle D|. \quad (\text{S7})$$

$$\hat{U}_{\text{pol}}^\dagger |A\rangle\langle B| \hat{U}_{\text{pol}} = e^{-\frac{i}{\hbar}\sqrt{\frac{2}{\hbar\omega_c^3}}\chi(\mu_{\text{AA}} - \mu_{\text{BB}})\hat{P}_c} |A\rangle\langle B|. \quad (\text{S8})$$

$$\hat{U}_{\text{pol}}^\dagger |B\rangle\langle A| \hat{U}_{\text{pol}} = e^{-\frac{i}{\hbar}\sqrt{\frac{2}{\hbar\omega_c^3}}\chi(\mu_{\text{BB}} - \mu_{\text{AA}})\hat{P}_c} |B\rangle\langle A|. \quad (\text{S9})$$

$$\hat{U}_{\text{pol}}^\dagger |D\rangle\langle D| \hat{U}_{\text{pol}} = |D\rangle\langle D|. \quad (\text{S10})$$

$$\hat{U}_{\text{pol}}^\dagger |B\rangle\langle B| \hat{U}_{\text{pol}} = |B\rangle\langle B|. \quad (\text{S11})$$

$$\hat{U}_{\text{pol}}^\dagger |A\rangle\langle A| \hat{U}_{\text{pol}} = |A\rangle\langle A|. \quad (\text{S12})$$

Using the result of Eq. S6 and Eq. S12 we find the following polaron transformation

$$\begin{aligned}
& \hat{U}_{\text{pol}}^\dagger \left[ \hat{Q}_c + \sqrt{\frac{2}{\hbar\omega_c^3}} \hat{\boldsymbol{\chi}} \cdot \hat{\boldsymbol{\mu}} \right] \hat{U}_{\text{pol}} \\
&= \hat{U}_{\text{pol}}^\dagger \hat{Q}_c \hat{U}_{\text{pol}} + \sqrt{\frac{2}{\hbar\omega_c^3}} \chi \hat{U}_{\text{pol}}^\dagger \left[ \mu_{\text{DB}} [|D\rangle\langle B| + |B\rangle\langle D|] + \mu_{\text{BA}} [|B\rangle\langle A| + |A\rangle\langle B|] \right. \\
&\quad \left. + \mu_{\text{DD}} |D\rangle\langle D| + \mu_{\text{BB}} |B\rangle\langle B| + \mu_{\text{AA}} |A\rangle\langle A| \right] \hat{U}_{\text{pol}} \\
&= \hat{Q}_c - \sqrt{\frac{2}{\hbar\omega_c^3}} \chi (\mu_{\text{DD}} |D\rangle\langle D| + \mu_{\text{BB}} |B\rangle\langle B| + \mu_{\text{AA}} |A\rangle\langle A|) + \sqrt{\frac{2}{\hbar\omega_c^3}} \chi \mu_{\text{DB}} \left[ e^{-\frac{i}{\hbar} \sqrt{\frac{2}{\hbar\omega_c^3}} \chi (\mu_{\text{DD}} - \mu_{\text{BB}}) \hat{P}_c} |D\rangle\langle B| \right. \\
&\quad \left. + e^{-\frac{i}{\hbar} \sqrt{\frac{2}{\hbar\omega_c^3}} \chi (\mu_{\text{BB}} - \mu_{\text{DD}}) \hat{P}_c} |B\rangle\langle D| \right] + \mu_{\text{BA}} \left[ e^{-\frac{i}{\hbar} \sqrt{\frac{2}{\hbar\omega_c^3}} \chi (\mu_{\text{BB}} - \mu_{\text{AA}}) \hat{P}_c} |B\rangle\langle A| + e^{-\frac{i}{\hbar} \sqrt{\frac{2}{\hbar\omega_c^3}} \chi (\mu_{\text{AA}} - \mu_{\text{BB}}) \hat{P}_c} |A\rangle\langle B| \right] \\
&\quad + \sqrt{\frac{2}{\hbar\omega_c^3}} \chi (\mu_{\text{DD}} |D\rangle\langle D| + \mu_{\text{BB}} |B\rangle\langle B| + \mu_{\text{AA}} |A\rangle\langle A|) \\
&= \hat{Q}_c + \sqrt{\frac{2}{\hbar\omega_c^3}} \chi \mu_{\text{DB}} \left[ e^{-\frac{i}{\hbar} \sqrt{\frac{2}{\hbar\omega_c^3}} \chi (\mu_{\text{DD}} - \mu_{\text{BB}}) \hat{P}_c} |D\rangle\langle B| + e^{-\frac{i}{\hbar} \sqrt{\frac{2}{\hbar\omega_c^3}} \chi (\mu_{\text{BB}} - \mu_{\text{DD}}) \hat{P}_c} |B\rangle\langle D| \right] \\
&\quad + \sqrt{\frac{2}{\hbar\omega_c^3}} \chi \mu_{\text{BA}} \left[ e^{-\frac{i}{\hbar} \sqrt{\frac{2}{\hbar\omega_c^3}} \chi (\mu_{\text{BB}} - \mu_{\text{AA}}) \hat{P}_c} |B\rangle\langle A| + e^{-\frac{i}{\hbar} \sqrt{\frac{2}{\hbar\omega_c^3}} \chi (\mu_{\text{AA}} - \mu_{\text{BB}}) \hat{P}_c} |A\rangle\langle B| \right] \quad (\text{S13})
\end{aligned}$$

With the above results, and the fact that  $e^{\hat{Y}}\hat{O}(\hat{X})e^{-\hat{Y}} = \hat{O}(e^{\hat{Y}}\hat{X}e^{-\hat{Y}})$  for a unitary operator  $e^{\hat{Y}}$ , we apply  $\hat{U}_{\text{pol}}$  to  $\hat{H}_{\text{PF}}$  and find the following polaron transformed PF Hamiltonian:

$$\begin{aligned}
\tilde{H}_{\text{PF}} &= \hat{U}_{\text{pol}}^\dagger \hat{H}_{\text{PF}} \hat{U}_{\text{pol}} = \hat{U}_{\text{pol}}^\dagger \hat{H}_{\text{m}} \hat{U}_{\text{pol}} + \frac{1}{2} \hat{P}_{\text{c}}^2 + \hat{U}_{\text{pol}}^\dagger \frac{1}{2} \omega_{\text{c}}^2 \left[ \hat{Q}_{\text{c}} + \sqrt{\frac{2}{\hbar \omega_{\text{c}}^3}} \hat{\boldsymbol{\chi}} \cdot \hat{\boldsymbol{\mu}} \right]^2 \hat{U}_{\text{pol}} \\
&= \hat{U}_{\text{pol}}^\dagger \hat{H}_{\text{m}} \hat{U}_{\text{pol}} + \frac{1}{2} \hat{P}_{\text{c}}^2 + \frac{1}{2} \omega_{\text{c}}^2 \left[ \hat{Q}_{\text{c}} + \sqrt{\frac{2}{\hbar \omega_{\text{c}}^3}} \chi \mu_{\text{DB}} \left[ e^{-\frac{i}{\hbar} \sqrt{\frac{2}{\hbar \omega_{\text{c}}^3}} \chi (\mu_{\text{DD}} - \mu_{\text{BB}}) \hat{P}_{\text{c}}} |D\rangle \langle B| \right. \right. \\
&\quad + e^{-\frac{i}{\hbar} \sqrt{\frac{2}{\hbar \omega_{\text{c}}^3}} \chi (\mu_{\text{BB}} - \mu_{\text{DD}}) \hat{P}_{\text{c}}} |B\rangle \langle D| \left. \left. + \sqrt{\frac{2}{\hbar \omega_{\text{c}}^3}} \chi \mu_{\text{BA}} \left[ e^{-\frac{i}{\hbar} \sqrt{\frac{2}{\hbar \omega_{\text{c}}^3}} \chi (\mu_{\text{BB}} - \mu_{\text{AA}}) \hat{P}_{\text{c}}} |B\rangle \langle A| \right. \right. \right. \\
&\quad \left. \left. \left. + e^{-\frac{i}{\hbar} \sqrt{\frac{2}{\hbar \omega_{\text{c}}^3}} \chi (\mu_{\text{AA}} - \mu_{\text{BB}}) \hat{P}_{\text{c}}} |A\rangle \langle B| \right] \right]^2 \\
&= \hat{U}_{\text{pol}}^\dagger \hat{H}_{\text{m}} \hat{U}_{\text{pol}} + \frac{1}{2} \hat{P}_{\text{c}}^2 + \frac{1}{2} \omega_{\text{c}}^2 \hat{Q}_{\text{c}}^2 + \frac{1}{\hbar \omega_{\text{c}}} \chi^2 \mu_{\text{DB}}^2 [|D\rangle \langle D| + |B\rangle \langle B|] + \frac{1}{\hbar \omega_{\text{c}}} \chi^2 \mu_{\text{BA}}^2 [|B\rangle \langle B| \\
&\quad + |A\rangle \langle A|] + \omega_{\text{c}}^2 \hat{Q}_{\text{c}} \sqrt{\frac{2}{\hbar \omega_{\text{c}}^3}} \chi \mu_{\text{DB}} \left[ e^{-\frac{i}{\hbar} \sqrt{\frac{2}{\hbar \omega_{\text{c}}^3}} \chi (\mu_{\text{DD}} - \mu_{\text{BB}}) \hat{P}_{\text{c}}} |D\rangle \langle B| + e^{-\frac{i}{\hbar} \sqrt{\frac{2}{\hbar \omega_{\text{c}}^3}} \chi (\mu_{\text{BB}} - \mu_{\text{DD}}) \hat{P}_{\text{c}}} |B\rangle \langle D| \right] \\
&\quad + \frac{1}{\hbar \omega_{\text{c}}} \chi^2 \mu_{\text{DB}} \mu_{\text{BA}} \left[ e^{-\frac{i}{\hbar} \sqrt{\frac{2}{\hbar \omega_{\text{c}}^3}} \chi (\mu_{\text{DD}} - \mu_{\text{AA}}) \hat{P}_{\text{c}}} |D\rangle \langle A| + e^{-\frac{i}{\hbar} \sqrt{\frac{2}{\hbar \omega_{\text{c}}^3}} \chi (\mu_{\text{AA}} - \mu_{\text{DD}}) \hat{P}_{\text{c}}} |A\rangle \langle D| \right] \\
&\quad + \omega_{\text{c}}^2 \hat{Q}_{\text{c}} \sqrt{\frac{2}{\hbar \omega_{\text{c}}^3}} \chi \mu_{\text{BA}} \left[ e^{-\frac{i}{\hbar} \sqrt{\frac{2}{\hbar \omega_{\text{c}}^3}} \chi (\mu_{\text{BB}} - \mu_{\text{AA}}) \hat{P}_{\text{c}}} |B\rangle \langle A| + e^{-\frac{i}{\hbar} \sqrt{\frac{2}{\hbar \omega_{\text{c}}^3}} \chi (\mu_{\text{AA}} - \mu_{\text{BB}}) \hat{P}_{\text{c}}} |A\rangle \langle B| \right] \\
&= \hat{U}_{\text{pol}}^\dagger \hat{H}_{\text{m}} \hat{U}_{\text{pol}} + (\hat{a}^\dagger \hat{a} + \frac{1}{2}) \hbar \omega_{\text{c}} + \frac{\hbar g_{\text{c}}^2}{\omega_{\text{c}}} [|D\rangle \langle D| + |B\rangle \langle B|] + \frac{\hbar \eta_{\text{c}}^2}{\omega_{\text{c}}} [|B\rangle \langle B| + |A\rangle \langle A|] \\
&\quad + \hbar g_{\text{c}} (\hat{a} + \hat{a}^\dagger) \left[ e^{-\frac{i}{\hbar} \sqrt{\frac{2}{\hbar \omega_{\text{c}}^3}} \chi (\mu_{\text{DD}} - \mu_{\text{BB}}) \hat{P}_{\text{c}}} |D\rangle \langle B| + e^{-\frac{i}{\hbar} \sqrt{\frac{2}{\hbar \omega_{\text{c}}^3}} \chi (\mu_{\text{BB}} - \mu_{\text{DD}}) \hat{P}_{\text{c}}} |B\rangle \langle D| \right] \\
&\quad + \frac{\hbar g_{\text{c}} \eta_{\text{c}}}{\omega_{\text{c}}} \left[ e^{-\frac{i}{\hbar} \sqrt{\frac{2}{\hbar \omega_{\text{c}}^3}} \chi (\mu_{\text{DD}} - \mu_{\text{AA}}) \hat{P}_{\text{c}}} |D\rangle \langle A| + e^{-\frac{i}{\hbar} \sqrt{\frac{2}{\hbar \omega_{\text{c}}^3}} \chi (\mu_{\text{AA}} - \mu_{\text{DD}}) \hat{P}_{\text{c}}} |A\rangle \langle D| \right] \\
&\quad + \hbar \eta_{\text{c}} (\hat{a} + \hat{a}^\dagger) \left[ e^{-\frac{i}{\hbar} \sqrt{\frac{2}{\hbar \omega_{\text{c}}^3}} \chi (\mu_{\text{BB}} - \mu_{\text{AA}}) \hat{P}_{\text{c}}} |B\rangle \langle A| + e^{-\frac{i}{\hbar} \sqrt{\frac{2}{\hbar \omega_{\text{c}}^3}} \chi (\mu_{\text{AA}} - \mu_{\text{BB}}) \hat{P}_{\text{c}}} |A\rangle \langle B| \right] \tag{S14}
\end{aligned}$$

From the second to third line of Eq. S14, we used the fact that,  $(\hat{a} + \hat{b} + \hat{c})^2 = (\hat{a} + \hat{b} + \hat{c}) \cdot (\hat{a} + \hat{b} + \hat{c})$ , where,

$$\begin{aligned}\hat{a} &= \hat{Q}_c, \\ \hat{b} &= \sqrt{\frac{2}{\hbar\omega_c^3}}\chi\mu_{DB} \left[ e^{-\frac{i}{\hbar}\sqrt{\frac{2}{\hbar\omega_c^3}}\chi(\mu_{DD}-\mu_{BB})\hat{P}_c} |D\rangle\langle B| + e^{-\frac{i}{\hbar}\sqrt{\frac{2}{\hbar\omega_c^3}}\chi(\mu_{BB}-\mu_{DD})\hat{P}_c} |B\rangle\langle D| \right], \\ \hat{c} &= \sqrt{\frac{2}{\hbar\omega_c^3}}\chi\mu_{BA} \left[ e^{-\frac{i}{\hbar}\sqrt{\frac{2}{\hbar\omega_c^3}}\chi(\mu_{BB}-\mu_{AA})\hat{P}_c} |B\rangle\langle A| + e^{-\frac{i}{\hbar}\sqrt{\frac{2}{\hbar\omega_c^3}}\chi(\mu_{AA}-\mu_{BB})\hat{P}_c} |A\rangle\langle B| \right].\end{aligned}\quad (\text{S15})$$

The fourth line of Eq. S14 is the final expression for the polaron transformed Hamiltonian of a DBA system where the cavity frequency is not in resonance with electronic transition. Note that, to proceed from the third to fourth line of Eq. S14 we used  $\hat{Q}_c = \sqrt{\frac{\hbar}{2\omega_c}}(\hat{a} + \hat{a}^\dagger)$ ,  $\hbar g_c = \chi\mu_{DB}$ , and  $\hbar\eta_c = \chi\mu_{BA}$ . Thus  $\hat{U}_{\text{pol}}^\dagger \hat{H}_m \hat{U}_{\text{pol}}$  is

$$\begin{aligned}\hat{U}_{\text{pol}}^\dagger \hat{H}_m \hat{U}_{\text{pol}} &= \frac{\hat{P}_s^2}{2M_s} + \sum_i \frac{1}{2} M_s \omega_s^2 (R_s - R_i^0)^2 |i\rangle\langle i| + \sum_i U_i |i\rangle\langle i| \\ &+ V_{DB} \left( e^{-\frac{i}{\hbar}\sqrt{\frac{2}{\hbar\omega_c^3}}\chi(\mu_{DD}-\mu_{BB})\hat{P}_c} |D\rangle\langle B| + e^{-\frac{i}{\hbar}\sqrt{\frac{2}{\hbar\omega_c^3}}\chi(\mu_{BB}-\mu_{DD})\hat{P}_c} |B\rangle\langle D| \right) \\ &+ V_{BA} \left( e^{-\frac{i}{\hbar}\sqrt{\frac{2}{\hbar\omega_c^3}}\chi(\mu_{BB}-\mu_{AA})\hat{P}_c} |B\rangle\langle A| + e^{-\frac{i}{\hbar}\sqrt{\frac{2}{\hbar\omega_c^3}}\chi(\mu_{AA}-\mu_{BB})\hat{P}_c} |A\rangle\langle B| \right) + \hat{H}_{\text{sb}}\end{aligned}\quad (\text{S16})$$

With this polaron transformed Hamiltonian in Eq. S14, we can extract the effective couplings between the donor and bridge ( $\tilde{V}_{n,l}^{\text{DB}}$ ), and the bridge and acceptor ( $\tilde{V}_{l,m}^{\text{BA}}$ ) state as follows

$$\begin{aligned}\tilde{V}_{n,l}^{\text{DB}} &= \langle D, n | \tilde{H}_{\text{PF}} - \hat{T}_s - \hat{H}_{\text{sb}} | B, l \rangle \\ &= \langle D, n | V_{DB} e^{-\frac{i}{\hbar}\sqrt{\frac{2}{\hbar\omega_c^3}}\chi(\mu_{DD}-\mu_{BB})\hat{P}_c} | D \rangle \langle B | B, l \rangle \\ &+ \hbar g_c \langle D, n | (\hat{a} + \hat{a}^\dagger) e^{-\frac{i}{\hbar}\sqrt{\frac{2}{\hbar\omega_c^3}}\chi(\mu_{DD}-\mu_{BB})\hat{P}_c} | D \rangle \langle B | B, l \rangle \\ &= V_{DB} S_{n,l}^{\text{DB}} + \hbar g_c [\sqrt{n} S_{n-1,l}^{\text{DB}} + \sqrt{n+1} S_{n+1,l}^{\text{DB}}]\end{aligned}\quad (\text{S17})$$

Similarly,

$$\begin{aligned}\tilde{V}_{l,m}^{\text{BA}} &= \langle \text{B}, l | \tilde{H}_{\text{PF}} - \hat{T}_{\text{S}} - \hat{H}_{\text{sb}} | \text{A}, m \rangle \\ &= V_{\text{BA}} S_{l,m}^{\text{BA}} + \hbar \eta_{\text{c}} [\sqrt{n} S_{l-1,m}^{\text{BA}} + \sqrt{l+1} S_{l+1,m}^{\text{BA}}]\end{aligned}\quad (\text{S18})$$

The direct donor to acceptor coupling is found to be:

$$\begin{aligned}\tilde{V}_{n,m}^{\text{DA}} &= \langle \text{D}, n | \tilde{H}_{\text{PF}} - \hat{T}_{\text{S}} - \hat{H}_{\text{sb}} | \text{A}, m \rangle \\ &= \frac{\hbar g_{\text{c}} \eta_{\text{c}}}{\omega_{\text{c}}} S_{n,m}^{\text{DA}}\end{aligned}\quad (\text{S19})$$

where,  $S_{n,l}^{\text{DB}} = \langle n | e^{-i/\hbar \sqrt{2/\hbar \omega_{\text{c}}^3} \chi (\mu_{\text{DD}} - \mu_{\text{BB}}) \hat{P}_{\text{c}}} | l \rangle$ ,  $S_{l,m}^{\text{BA}} = \langle l | e^{-i/\hbar \sqrt{2/\hbar \omega_{\text{c}}^3} \chi (\mu_{\text{BB}} - \mu_{\text{AA}}) \hat{P}_{\text{c}}} | m \rangle$ , and  $S_{n,m}^{\text{DA}} = \langle n | e^{-i/\hbar \sqrt{2/\hbar \omega_{\text{c}}^3} \chi (\mu_{\text{DD}} - \mu_{\text{AA}}) \hat{P}_{\text{c}}} | m \rangle$

The bridge mediated effective donor-acceptor coupling ( $V_{n,m}^{\text{DA}}$ ) can be calculated by perturbative technique i.e. the transformation method,<sup>?</sup> and

$$\tilde{V}_{n,m}^{\text{DA}} = - \sum_l \frac{\tilde{V}_{nl}^{*\text{DB}} \tilde{V}_{l,m}^{\text{BA}}}{2} \left[ \frac{1}{(U_{\text{B}} - U_{\text{A}}) + (l - m) \hbar \omega_{\text{c}}} + \frac{1}{(U_{\text{B}} - U_{\text{D}}) + (l - n) \hbar \omega_{\text{c}}} \right] \quad (\text{S20})$$

Hence, the total DA coupling is:

$$\begin{aligned}F_{n,m}^{\text{DA}} &= \tilde{V}_{n,m}^{\text{DA}} + \tilde{V}_{n,m}^{\text{DA}'} \\ &= \frac{\hbar g_{\text{c}} \eta_{\text{c}}}{\omega_{\text{c}}} S_{n,m}^{\text{DA}} - \sum_l \frac{\tilde{V}_{nl}^{*\text{DB}} \tilde{V}_{l,m}^{\text{BA}}}{2} \left[ \frac{1}{(U_{\text{B}} - U_{\text{A}}) + (l - m) \hbar \omega_{\text{c}}} + \frac{1}{(U_{\text{B}} - U_{\text{D}}) + (l - n) \hbar \omega_{\text{c}}} \right]\end{aligned}\quad (\text{S21})$$

With the above polaron transformation, the polaron mediated electron transfer (PMET) rate is:

$$k_{\text{FGR}} = \sum_n P_n \sum_m \frac{|F_{n,m}^{\text{DA}}|^2}{\hbar} \sqrt{\frac{\pi}{\lambda_{\text{DA}} k_{\text{B}} T}} \exp \left[ - \frac{(\Delta G_{n,m} + \lambda_{\text{DA}})^2}{4 \lambda_{\text{DA}} k_{\text{B}} T} \right], \quad (\text{S22})$$

where,  $\Delta G_{n,m}$  is the effective driving force for each channel

$$\begin{aligned} \Delta G_{n,m} = & -(U_D - U_A) + (m - n)\hbar\omega_c - \sum_l \frac{(\tilde{V}_{l,n}^{\text{BA}})^{\text{T}} \tilde{V}_{l,m}^{\text{BA}}}{(U_B - U_A) + (l - m)\hbar\omega_c} \\ & + \sum_l \frac{(\tilde{V}_{n,l}^{\text{DB}})(\tilde{V}_{m,l}^{\text{DB}})^{\text{T}}}{(U_B - U_D) + (l - n)\hbar\omega_c} \end{aligned} \quad (\text{S23})$$

with,

$$P_n = \frac{\exp[-\beta n\hbar\omega_c]}{\sum_n \exp[-\beta n\hbar\omega_c]}. \quad (\text{S24})$$

### Derivation of the PMET Rate for the On-Resonance Case

As in the previous section, we introduce the following polaron transformation of the photonic DOF

$$\hat{U}_{\text{pol}} = \exp \left[ \frac{i}{\hbar} \sqrt{\frac{2}{\hbar\omega_c^3}} \chi \sum_{j \in \text{D,A}} \mu_{jj} |j\rangle \langle j| \hat{P}_c \right]. \quad (\text{S25})$$

In this system the bridge state is not coupled with the light field. Following the same derivation as described in the previous section, we find:

$$\begin{aligned} \tilde{H}_{\text{PF}} = \hat{U}_{\text{pol}}^\dagger \hat{H}_{\text{PF}} \hat{U}_{\text{pol}} &= \hat{U}_{\text{pol}}^\dagger \hat{H}_m \hat{U}_{\text{pol}} + \frac{1}{2} \hat{P}_c^2 + \hat{U}_{\text{pol}}^\dagger \frac{1}{2} \omega_c^2 \left[ \hat{Q}_c + \sqrt{\frac{2}{\hbar\omega_c^3}} \hat{\boldsymbol{\chi}} \cdot \hat{\boldsymbol{\mu}} \right]^2 \hat{U}_{\text{pol}} \\ &= \hat{U}_{\text{pol}}^\dagger \hat{H}_m \hat{U}_{\text{pol}} + \frac{1}{2} \hat{P}_c^2 + \frac{1}{2} \omega_c^2 \left[ \hat{Q}_c + \sqrt{\frac{2}{\hbar\omega_c^3}} \chi \mu_{\text{DA}} \left( e^{\frac{i}{\hbar} \sqrt{\frac{2}{\hbar\omega_c^3}} \chi \Delta \mu \hat{P}_c} \hat{\sigma}^\dagger + e^{-\frac{i}{\hbar} \sqrt{\frac{2}{\hbar\omega_c^3}} \chi \Delta \mu \hat{P}_c} \hat{\sigma} \right) \right]^2 \\ &= \hat{U}_{\text{pol}}^\dagger \hat{H}_m \hat{U}_{\text{pol}} + \left( \hat{a}^\dagger \hat{a} + \frac{1}{2} \right) \hbar\omega_c + \hbar g_c (\hat{a}^\dagger + \hat{a}) \left( e^{\frac{i}{\hbar} \sqrt{\frac{2}{\hbar\omega_c^3}} \chi \Delta \mu \hat{P}_c} \hat{\sigma}^\dagger + e^{-\frac{i}{\hbar} \sqrt{\frac{2}{\hbar\omega_c^3}} \chi \Delta \mu \hat{P}_c} \hat{\sigma} \right) + \frac{\hbar g_c^2}{\omega_c} \hat{\mathbf{1}}_e. \end{aligned} \quad (\text{S26})$$



where  $\Delta\mu = \mu_{\text{DD}} - \mu_{\text{AA}}$ ,  $\hat{\sigma}^\dagger = |\text{A}\rangle\langle\text{D}|$ ,  $\hat{\sigma} = |\text{D}\rangle\langle\text{A}|$ ,  $\hat{1}_e = |\text{D}\rangle\langle\text{D}| + |\text{A}\rangle\langle\text{A}|$ , and  $\hbar g_c = \chi\mu_{\text{DA}}$ . Finally,  $\hat{U}_{\text{pol}}^\dagger \hat{H}_m \hat{U}_{\text{pol}}$  is

$$\begin{aligned} \hat{U}_{\text{pol}}^\dagger \hat{H}_m \hat{U}_{\text{pol}} &= \frac{\hat{P}_s^2}{2M_s} + \sum_i \frac{1}{2} M_s \omega_s^2 (R_s - R_i^0)^2 |i\rangle\langle i| + \sum_i U_i |i\rangle\langle i| \\ &+ V_{\text{DB}} (e^{-\frac{i}{\hbar} \sqrt{\frac{2}{\hbar\omega_c^3}} \chi \mu_{\text{DD}} \hat{P}_c} |\text{D}\rangle\langle\text{B}| + e^{\frac{i}{\hbar} \sqrt{\frac{2}{\hbar\omega_c^3}} \chi \mu_{\text{DD}} \hat{P}_c} |\text{B}\rangle\langle\text{D}|) \\ &+ V_{\text{BA}} (e^{\frac{i}{\hbar} \sqrt{\frac{2}{\hbar\omega_c^3}} \chi \mu_{\text{AA}} \hat{P}_c} |\text{B}\rangle\langle\text{A}| + e^{-\frac{i}{\hbar} \sqrt{\frac{2}{\hbar\omega_c^3}} \chi \mu_{\text{AA}} \hat{P}_c} |\text{A}\rangle\langle\text{B}|) + \hat{H}_{\text{sb}} \end{aligned} \quad (\text{S27})$$

With the polaron transformed Hamiltonian in Eq. S26, we can compute the effective couplings between the donor and bridge ( $\tilde{V}_{n,l}^{\text{DB}}$ ), and the bridge and acceptor ( $\tilde{V}_{l,m}^{\text{BA}}$ ) states as follows:

$$\begin{aligned} \tilde{V}_{n,0}^{\text{DB}} &= \langle \text{D}, n | \tilde{H}_{\text{PF}} - \hat{T}_s - \hat{H}_{\text{sb}} | \text{B}, 0 \rangle \\ &= \langle \text{D}, n | V_{\text{DB}} e^{-\frac{i}{\hbar} \sqrt{\frac{2}{\hbar\omega_c^3}} \chi \mu_{\text{DD}} \hat{P}_c} | \text{D} \rangle \langle \text{B} | \text{B}, 0 \rangle \\ &= V_{\text{DB}} S_{n,0}^{\text{DB}} \end{aligned} \quad (\text{S28})$$

Similarly,

$$\begin{aligned} \tilde{V}_{0,m}^{\text{BA}} &= \langle \text{B}, 0 | \tilde{H}_{\text{PF}} - \hat{T}_s - \hat{H}_{\text{sb}} | \text{A}, m \rangle \\ &= V_{\text{BA}} S_{0,m}^{\text{BA}} \end{aligned} \quad (\text{S29})$$

The direct donor to acceptor coupling is:

$$\begin{aligned} \tilde{V}_{nm}^{\text{DA}} &= \langle \text{D}, n | \tilde{H}_{\text{PF}} - \hat{T}_s - \hat{H}_{\text{sb}} | \text{A}, m \rangle \\ &= \hbar g_c [\sqrt{n} S_{n-1,m} + \sqrt{n+1} S_{n+1,m}] \end{aligned} \quad (\text{S30})$$

where,  $S_{n,0}^{\text{DB}} = \langle n | e^{-i/\hbar \sqrt{2/\hbar\omega_c^3} \chi \mu_{\text{DD}} \hat{P}_c} | 0 \rangle$ ,  $S_{0,m}^{\text{BA}} = \langle 0 | e^{i/\hbar \sqrt{2/\hbar\omega_c^3} \chi \mu_{\text{AA}} \hat{P}_c} | m \rangle$ , and  $S_{n,m}^{\text{DA}} = \langle n | e^{-i/\hbar \sqrt{2/\hbar\omega_c^3} \chi (\mu_{\text{DD}} - \mu_{\text{AA}}) \hat{P}_c} | m \rangle$ .

We again calculate the through-bridge interactions using the transformation method.<sup>?</sup>

The indirect coupling between donor and acceptor state is:

$$\tilde{V}'_{n,m}{}^{\text{DA}} = -\frac{\tilde{V}_{n0}^{*\text{DB}}\tilde{V}_{0m}^{\text{BA}}}{2} \left[ \frac{1}{(U_{\text{B}} - U_{\text{A}}) - m\hbar\omega_c} + \frac{1}{(U_{\text{B}} - U_{\text{D}}) - n\hbar\omega_c} \right] \quad (\text{S31})$$

Hence, the total donor to acceptor coupling is:

$$\begin{aligned} F_{n,m}^{\text{DA}} &= \tilde{V}_{n,m}^{\text{DA}} + \tilde{V}'_{n,m}{}^{\text{DA}} \\ &= \hbar g_c [\sqrt{n}S_{n-1,m} + \sqrt{n+1}S_{n+1,m}] - \frac{\tilde{V}_{n,0}^{\text{DB}}\tilde{V}_{0,m}^{\text{BA}}}{2} \left[ \frac{1}{(U_{\text{B}} - U_{\text{A}}) - m\hbar\omega_c} + \frac{1}{(U_{\text{B}} - U_{\text{D}}) - n\hbar\omega_c} \right], \end{aligned} \quad (\text{S32})$$

which is found in Eq. (7) of the main text. Finally, the polariton mediated electron transfer (PMET) rate is:

$$k_{\text{FGR}} = \sum_n P_n \sum_m \frac{|V_{nm}^{\text{DA}}|^2}{\hbar} \sqrt{\frac{\pi}{\lambda_{\text{DA}} k_{\text{B}} T}} \exp \left[ -\frac{(\Delta G_{nm} + \lambda_{\text{DA}})^2}{4\lambda_{\text{DA}} k_{\text{B}} T} \right], \quad (\text{S33})$$

where,  $\Delta G_{nm}$  is the effective driving force for each channel

$$\Delta G_{nm} = -(U_{\text{D}} - U_{\text{A}}) + (m - n)\hbar\omega_c - \frac{(\tilde{V}_{0,n}^{\text{BA}})^{\text{T}}\tilde{V}_{0,m}^{\text{BA}}}{(U_{\text{B}} - U_{\text{A}}) - m\hbar\omega_c} + \frac{\tilde{V}_{n,0}^{\text{DB}}(\tilde{V}_{m,0}^{\text{DB}})^{\text{T}}}{(U_{\text{B}} - U_{\text{D}}) - n\hbar\omega_c} \quad (\text{S34})$$

with,

$$P_n = \frac{\exp[-\beta n\hbar\omega_c]}{\sum_n \exp[-\beta n\hbar\omega_c]}. \quad (\text{S35})$$

## Additional Numerical Results

Here, we present additional numerical results for polariton mediated electron transfer (PMET) in the off-resonance limit. We describe the PMET rate obtained from the FGR rate expression (Eq. S22). Figure S1(A) and S1(B) show the computed PMET rates as a function of the donor-bridge energy gap  $\Delta E = U_{\text{B}} - U_{\text{D}}$  at a high cavity frequency ( $\hbar\omega_c = 200$  meV) and at a low cavity frequency ( $\hbar\omega_c = 40$  meV). We set  $g_c$  and  $\eta_c$  to be equal, where  $\hbar g_c = \chi\mu_{\text{DB}}$ ,

$$\hbar\eta_c = \chi\mu_{BA}.$$

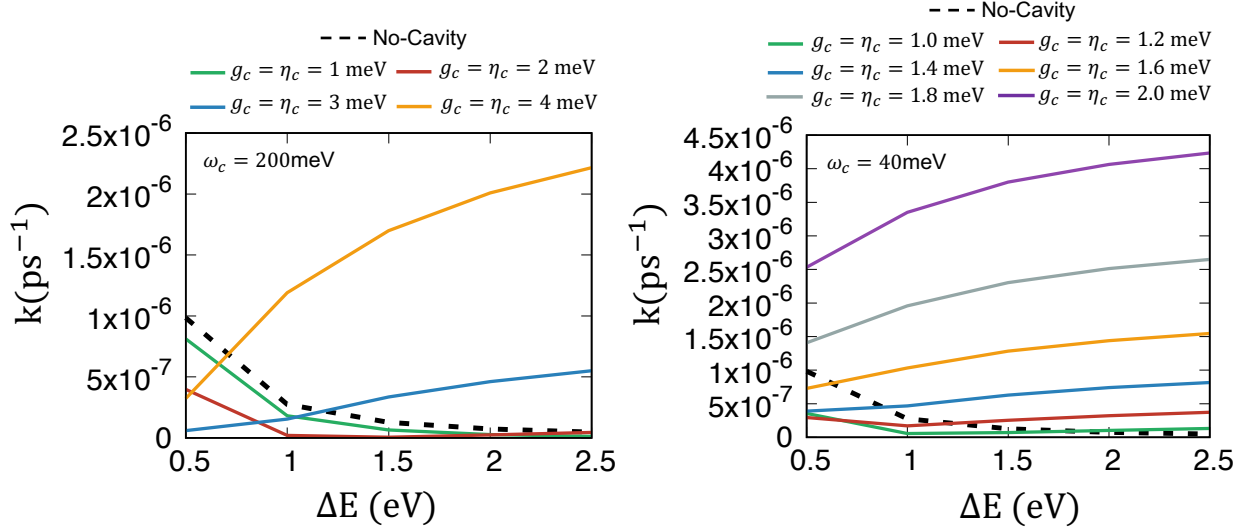


Figure S1: PMET rate constant obtained over a range of  $\Delta E = U_B - U_D$  for off resonance condition with (A)  $\hbar\omega_c = 200$  meV and (B)  $\hbar\omega_c = 40$  meV. Different colored lines correspond to different light-matter interaction strength.

When the molecule is decoupled from the cavity, the electron transfer occurs via the  $|D\rangle \rightarrow |B\rangle \rightarrow |A\rangle$  superexchange pathway and one finds that the ET rate decreases with  $\Delta E = U_B - U_D$ . This is understood by analyzing at the donor-acceptor coupling  $V_{DA}^{\text{eff}}$ , which is inversely proportional to the donor-bridge energy gap (see Eq. (6) of the main text). With a cavity, ET is mediated by two different coupling pathways (as described in the main text)

- **Pathway 1:** ET from photon dressed donor states  $|D, n\rangle$  to photon dressed acceptor states  $|A, m\rangle$  via bridge mediated channels  $|B, l\rangle$ .
- **Pathway 2:** ET from direct transitions between  $|D, n\rangle$  to  $|A, m\rangle$ . This direct transition is controlled by the cavity properties, such as the light-matter coupling strengths and the photon frequency.

Figure S1(A) shows the computed PMET rate for a high photon frequency ( $\hbar\omega_c = 200$  meV,  $\hbar\omega_c \gg k_B T$ ). In this regime, only  $|D, 0\rangle$  has appreciable thermal population. Hence, the predominant reactive channels are  $|D, 0\rangle \rightarrow \sum_l |B, l\rangle \rightarrow \{|A, 0\rangle, |A, 1\rangle\}$  via pathways

(1), (bridge mediated), and  $|D, 0\rangle \rightarrow \{|A, 0\rangle, |A, 1\rangle\}$  via pathways (2), (direct transitions from donor to acceptor). The higher energy acceptor states  $|A, 2\rangle, |A, 3\rangle\dots$  are energetically disfavored due to their reduced Franck-Condon factors. At relatively low  $\Delta E$  ( $\sim 0.5\text{-}1$  eV), these two pathway interfere destructively, so the overall rate is smaller compared to the cavity free scenario. Increasing  $\Delta E$  causes the charge transfer to occur mostly via pathway (2), so the destructive interference is reduced and the reaction rate is enhanced. This rate enhancement is proportional to the light-matter coupling strength, as indicated in the figure. The rate enhancement can also be understood from Eq. S21. The first term in Eq. S21 describes the direct transition from donor to acceptor, and this term grows with increasing light-matter coupling. For smaller  $\Delta E$  values, the ET rate decreases due to the larger destructive interference between pathways (1) and (2). Strong light-matter coupling can overcome this destructive interference and boost the overall rate. For instance, Figure S1(A) shows that at  $\Delta E = 0.5\text{-}1.0$  eV, and  $g_c = \eta_c > 2$  meV, the rates are largely enhanced in comparison with the case of  $g_c = \eta_c \leq 2$  meV.

Figure S1(B) shows the PMET rate at low photon frequency ( $\hbar\omega_c = 40$  meV,  $\hbar\omega_c \ll k_B T$ ). The fundamental difference is that the high lying donor dressed states (i.e.,  $|D, 1\rangle, |D, 2\rangle, |D, 3\rangle\dots$ ) are initially populated or have appreciable thermal population. Thus, these high-lying channels can participate in the ET reaction. The significant difference is that, at low photon frequency, the destructive interference is larger compare to the case with high photon frequencies. For example, for comparable effective light-matter coupling strengths ( $g_c/\omega_c$ ), with  $g_c = 4.0$  meV ( $g_c/\omega_c \simeq 0.02$ ) in Figure S1(A) and  $g_c = 1.0$  meV ( $g_c/\omega_c \simeq 0.025$ ) in Figure S1(B), the overall rate profile for Figure S1(B) is much smaller in magnitude compared to the data in Figure S1(A). This difference in the rate profiles arises from the multiple-donor dressed states that induce destructive interference for low photon frequency (Figure S1(B)) that is more pronounced over a wide range of  $\Delta E$ .